# Kinematics Analyzing of a Spatial Multi-Section Continuum Robot

Duong Xuan Bien[1], Chu Anh My[1], Nguyen Van Cong[1], Do Tien Lap[1], and Tran Van Hieu[2]

[1]Le Quy Don Technical University,
No. 236, Hoang Quoc Viet Street, Cau Giay District, Vietnam
E-mail: xuanbien82@yahoo.com
[2]Engineering Intermediate School-General Technical Department

**Abstract**

Over the past several years, a new class of robots, known as soft robots has been studied by a number of researchers. One of the types of the soft robots is continuum robot which has high degree of freedom or continuous, backbone structures. In this article, a spatial multi-section continuum robot with elastic backbone are considered. The forward and inverse kinematics problem of a spatial three-section continuum robot are solved as the illustrative example. Forward kinematics is the first step towards solving the inverse kinematics and dynamics problem. Inverse kinematics problem plays important role in designing the control system for robots.

*Keywords*: Kinematic modeling, continuum robots, forward kinematics, inverse kinematics.

## 1. Introduction

Soft and continuum robots driven by tendons or cables have wide-ranging applications. Smooth and complex motion, continuum robots can change the shape and compatibility when interacting with human. They have great potential in medicine [1], [2].

A continuum robot which uses an elastic backbone consisting of three circular sections is shown in Fig. 1. It is controlled by secondary backbones or driving cables [3], [4], [5], [6], or tendon [7], [8], [9], [10], [11].
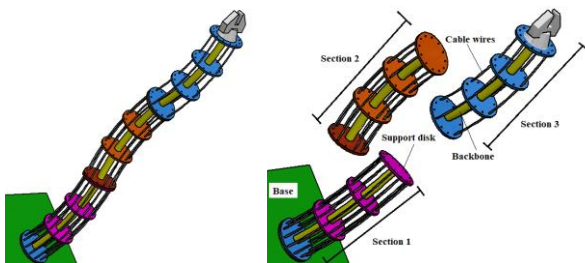


Figure 1. A spatial three-section continuum robot

The kinematic and dynamic equations of continuum robots are built by using the Hamilton equations [12], Elliptical integration [13], Cosserat beam theory [3], [7], [14], [15], [16], Virtual power [8] or Ritz-Galerkin [17].

The continuum robots have complex structure and many degree of freedom (DOFs). For example, a section of the spatial continuum robot has at least two DOFs. The number of DOF is much larger than the minimum required to perform the task in the workspace. This means the spatial continuum robot is a redundant system. Although redundant characteristic helps robot moving smoothly and flexibly. This residual movement creates many difficulties in kinematics and dynamics modeling. In particular, the first difficulty is the inverse kinematics problem. The kinematic modeling and the inverse kinematic problem are presented for a spatial continuum robot based on D-H techniques [18]. Inverse kinematics is solved by using the optimal algorithm SQP for a class of continuum bionic handling arm [19]. The modeling approach is inspired from a model of a hyper-redundant backbone-based manipulator. Newton Rapson iterative and Damp Least Square method are used to solve inverse kinematic directly using forward kinematic model [20]. A heuristic approach to iteratively solve the inverse kinematics problem of a continuum robot is proposed [21]. Some simulation results show that the algorithm is highly effective in computing with different topologies.

In this paper, a spatial multi-section continuum robot is considered. The kinematics modeling of this robot is presented through building the kinematic equations of the backbone. Based on these equations, the forward and inverse kinematics problem of spatial three-section continuum robot are analyzed. The inverse kinematics is solved using the Jacobian method with pseudoinverse matrix combining the closed-loop algorithm at the velocity level. The results of this research can be used for considering the other continuum robot such as varied multi-section, more numbers of degree of freedom and build the dynamics equations and design the control system.

## 2. Kinematic modeling

Firstly, considering the two-section continuum robot as Fig. 2. Assume that the curvature is constant within each section. Where, $(OXYZ)_0$ is the fixed coordinate

system. The $(OXYZ)_1$ and $(OXYZ)_2$ are the local coordinate systems which are attached to the section 1 and section 2, respectively. The origin of local frame is always at the first point of each section. Axes $(OZ)_1$ and $(OZ)_2$ are tangent to the arc of the corresponding sections. The contact point is the origin of frame. $C_1$ and $C_2$ are centre of curvatures of arcs section 1 and 2. These centres are always on the local $(OX)_1$ and $(OX)_2$. The other axes are determined by the right-hand rule.
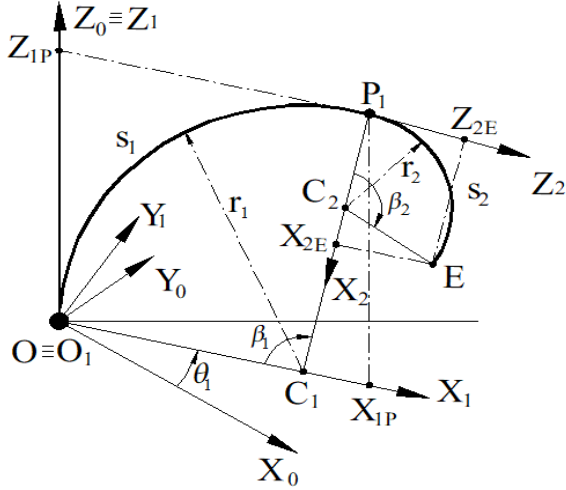


Figure. 2. A two-section backbone of a spatial continuum robot

The parameters of bending arc are related to each other according to formula as below

$$\beta_i(t) = s_i(t)\kappa_i(t); i = 1,2,3 \tag{1}$$

Where $s_i(t)$ is the length of arc $i$. The position vector of the section 1 endpoint (point P) in the local frame $(OXYZ)_1$ is determined as

$$\mathbf{r}_{1P} = \left[ \frac{1}{\kappa_1}(1 - \cos\beta_1) \quad 0 \quad \frac{1}{\kappa_1}\sin\beta_1 \right]^T \tag{2}$$

The position of this point in the fixed frame $(OXYZ)_0$

$$\mathbf{r}_{01} = \mathbf{T}_1\mathbf{r}_{1P} = \begin{bmatrix} \dfrac{1}{\kappa_1}(1 - \cos\beta_1)\cos\theta_1 \\ \dfrac{1}{\kappa_1}(1 - \cos\beta_1)\sin\theta_1 \\ \dfrac{1}{\kappa_1}\sin\beta_1 \end{bmatrix} \tag{3}$$

where $\mathbf{T}_1$ is the rotational matrix around $(OZ)_1$

$$\mathbf{T}_1 = \begin{bmatrix} \cos\theta_1 & -\sin\theta_1 & 0 \\ \sin\theta_1 & \cos\theta_1 & 0 \\ 0 & 0 & 1 \end{bmatrix} \tag{4}$$

Similarly, the position vector of end-effector point (point E) in frame $(OXYZ)_2$ is calculated as

$$\mathbf{r}_{2E} = \left[ \frac{1}{\kappa_2}(1 - \cos\beta_2) \quad 0 \quad \frac{1}{\kappa_2}\sin\beta_2 \right]^T \tag{5}$$

To determine the position vector of end-effector point in fixed frame $(OXYZ)_0$, the steps are executed as follow

- Rotate the frame $(OXYZ)_2$ around axis $OZ_2$ with angle $\theta_2$, we have the rotational matrix

$$\mathbf{T}_2 = \begin{bmatrix} \cos\theta_2 & -\sin\theta_2 & 0 \\ \sin\theta_2 & \cos\theta_2 & 0 \\ 0 & 0 & 1 \end{bmatrix} \tag{6}$$

- Rotate the frame received around axis $OY_1$ with angle $\beta_1$, the rotational matrix is described as

$$\mathbf{T}_{1Y} = \begin{bmatrix} \cos\beta_1 & 0 & \sin\beta_1 \\ 0 & 1 & 0 \\ -\sin\beta_1 & 0 & \cos\beta_1 \end{bmatrix} \tag{7}$$

- Rotate the new frame around axis $OZ_1$ with angle $\theta_1$ follow the matrix in (4).

The position vector of end-effector in fixed frame is calculated as

$$\mathbf{r}_{02} = \mathbf{r}_{01} + \mathbf{T}_1\mathbf{T}_{1Y}\mathbf{T}_2\mathbf{r}_{02} = \begin{bmatrix} r_{02x} & r_{02y} & r_{02z} \end{bmatrix}^T \tag{8}$$

Specific coordinates can be shown as

$$r_{02x} = \frac{1}{\kappa_1}(1-\cos\beta_1)\cos\theta_1 + \frac{1}{\kappa_2}(\cos\beta_1\cos\theta_1\cos\theta_2 - \sin\theta_1\sin\theta_2)(1-\cos\beta_2) + \frac{1}{\kappa_2}\sin\beta_1\sin\beta_2\cos\theta_1$$

$$r_{02y} = \frac{1}{\kappa_1}(1-\cos\beta_1)\sin\theta_1 + \frac{1}{\kappa_2}(\cos\beta_1\sin\theta_1\cos\theta_2 - \cos\theta_1\sin\theta_2)(1-\cos\beta_2) + \frac{1}{\kappa_2}\sin\beta_1\sin\beta_2\sin\theta_1 \tag{9}$$

$$r_{02z} = \frac{1}{\kappa_1}\sin\beta_1 - \frac{1}{\kappa_2}\sin\beta_1\cos\theta_2(1-\cos\beta_2) + \frac{1}{\kappa_2}\cos\beta_1\sin\beta_2$$

With the similar analysing, the end-effector coordinates of a spatial three-section continuum robot in $(OXYZ)_0$ can be determined as

$$
\begin{aligned}
xE := & \frac{\cos(\theta1)\,(1-\cos(\beta1))}{k1} + \frac{(\cos(\theta1)\cos(\beta1)\cos(\theta2) - \sin(\theta1)\sin(\theta2))\,(1-\cos(\beta2))}{k2} + \frac{\cos(\theta1)\sin(\beta1)\sin(\beta2)}{k2} \\
& + \frac{1}{k3}((((\cos(\theta1)\cos(\beta1)\cos(\theta2) - \sin(\theta1)\sin(\theta2))\cos(\beta2) - \cos(\theta1)\sin(\beta1)\sin(\theta2))\cos(\theta3) + (-\cos(\theta1)\cos(\beta1)\sin(\theta2) \\
& - \sin(\theta1)\cos(\theta2))\sin(\theta3))\,(1-\cos(\beta3))) + \frac{((\cos(\theta1)\cos(\beta1)\cos(\theta2) - \sin(\theta1)\sin(\theta2))\sin(\beta2) + \cos(\theta1)\sin(\beta1)\cos(\beta2))\sin(\beta3)}{k3}
\end{aligned}
$$

$$
\begin{aligned}
yE := & \frac{\sin(\theta1)\,(1-\cos(\beta1))}{k1} + \frac{(\sin(\theta1)\cos(\beta1)\cos(\theta2) + \cos(\theta1)\sin(\theta2))\,(1-\cos(\beta2))}{k2} + \frac{\sin(\theta1)\sin(\beta1)\sin(\beta2)}{k2} \\
& + \frac{1}{k3}((((\sin(\theta1)\cos(\beta1)\cos(\theta2) + \cos(\theta1)\sin(\theta2))\cos(\beta2) - \sin(\theta1)\sin(\beta1)\sin(\theta2))\cos(\theta3) + (-\sin(\theta1)\cos(\beta1)\sin(\theta2) \\
& + \cos(\theta1)\cos(\theta2))\sin(\theta3))\,(1-\cos(\beta3))) + \frac{((\sin(\theta1)\cos(\beta1)\cos(\theta2) + \cos(\theta1)\sin(\theta2))\sin(\beta2) + \sin(\theta1)\sin(\beta1)\cos(\beta2))\sin(\beta3)}{k3}
\end{aligned}
\tag{10}
$$

$$
\begin{aligned}
zE := & \frac{\sin(\beta1)}{k1} - \frac{\sin(\beta1)\cos(\theta2)\,(1-\cos(\beta2))}{k2} + \frac{\cos(\beta1)\sin(\beta2)}{k2} + \frac{(-\sin(\beta1)\cos(\theta2)\sin(\beta2) + \cos(\beta1)\cos(\beta2))\sin(\beta3)}{k3} \\
& + \frac{((-\sin(\beta1)\cos(\theta2)\cos(\beta2) - \cos(\beta1)\sin(\beta2))\cos(\theta3) + \sin(\beta1)\sin(\theta2)\sin(\theta3))\,(1-\cos(\beta3))}{k3}
\end{aligned}
$$

Consider a spatial $n$-section continuum robot, the position vector of end-effector in $(OXYZ)_0$ is given as

$$\mathbf{r}_{0E} = \mathbf{r}_{0(n-1)} + \mathbf{T}_1\mathbf{T}_{1y}\mathbf{T}_2...\mathbf{T}_{n-1}\mathbf{T}_{(n-1)y}\mathbf{T}_n\mathbf{r}_{nE} \tag{11}$$

# 3. Kinematic analyzing

In this section, the forward and inverse kinematics problem of spatial three-section continuum robot are analyzed.

## 3.1. Forward kinematics analyzing

Forward kinematics is the first step towards solving the inverse kinematics and dynamics problem. The lengths of three sections sequence are $L_1 = 0.3(m); L_2 = 0.5(m); L_3 = 0.7(m)$ and $L_{03} = 0.7(m)$. The joint variables of sections are given as (12). Fig. 3, Fig. 4 and Fig. 5 show the values of curvature of three sections, respectively.

$$
\begin{aligned}
Section1: &\quad \kappa_1 = 1 + 0.2\sin(\frac{\pi}{2}t) \ (m^{-1}); \quad \beta_1 = 0.5\cos(\frac{\pi}{2}t) \ (rad); \quad \theta_1 = \sin(\frac{\pi}{2}t) \ (rad) \\
Section2: &\quad \kappa_2 = 0.8 + 0.1\sin(\frac{\pi}{3}t) \ (m^{-1}); \quad \beta_2 = 0.5\cos(\frac{\pi}{3}t) \ (rad); \quad \theta_2 = 0.5\sin(\frac{\pi}{3}t) \ (rad) \\
Section3: &\quad \kappa_3 = 0.5 + 0.1\sin(\frac{\pi}{4}t) \ (m^{-1}); \quad \beta_3 = 0.3\cos(\frac{\pi}{4}t) \ (rad); \quad \theta_3 = 0.3\sin(\frac{\pi}{4}t) \ (rad)
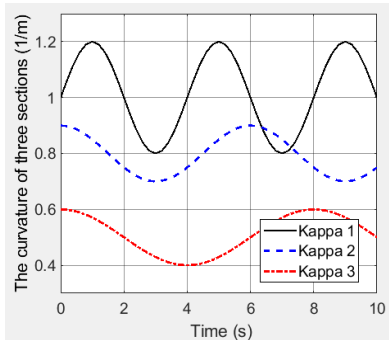\end{aligned}
\tag{12}
$$



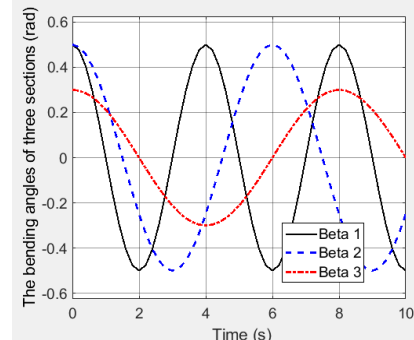Figure 3. The curvature values of three sections



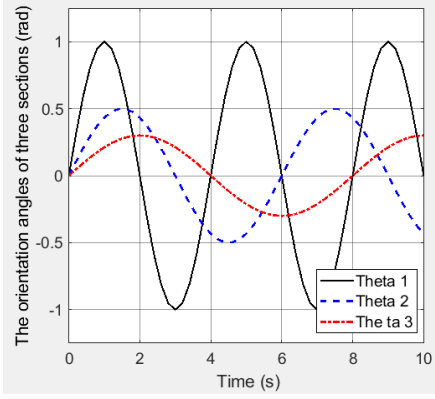Figure 4. The bending angle values of three sections

Figure 5. The orientation angle values of three sections

Fig. 6 shows the diagram to solve forward kinematics problem for continuum robots. The results are the positions and velocity of the endpoint which are described in Fig. 7 and Fig. 8.
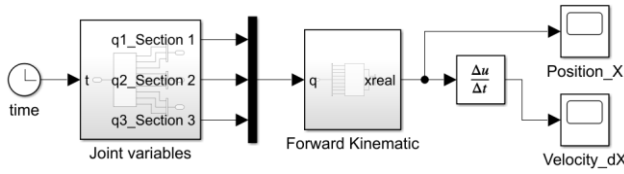


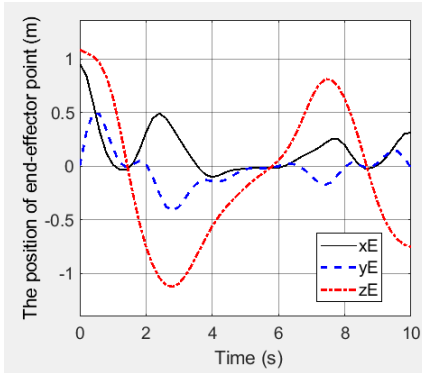Figure 6. Solving forward kinematics problem in SIMULINK
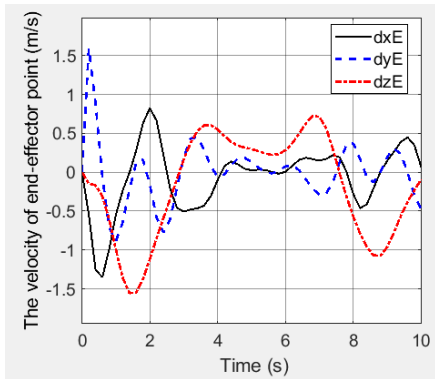


Figure 7. The endpoint position in workspace



Figure 8. The endpoint velocity in workspace

### 3.2. Inverse kinematics analyzing

Assume that the path $\mathbf{x}_d(t), \dot{\mathbf{x}}_d(t)$ in workspace is given. The goal is to find the joint variables in joint space $\mathbf{q}(t), \dot{\mathbf{q}}(t)$ that reproduce the given path. Define

the joint variable vector for a $n$-section spatial continuum robot as

$$\mathbf{q}(t) = \begin{bmatrix} \mathbf{q}_1^T & \mathbf{q}_2^T & ... & \mathbf{q}_n^T \end{bmatrix}^T \tag{13}$$

where, $\mathbf{q}_i = \begin{bmatrix} \kappa_i & \beta_i & \theta_i \end{bmatrix}; i = 1 \div n$ is the joint variables vector of section $i$.

The forward kinematic equations can be given as

$$\mathbf{x} = f(\mathbf{q}) \tag{14}$$

The differential kinematics equation is described as

$$\dot{\mathbf{x}} = \mathbf{J}(\mathbf{q})\dot{\mathbf{q}} \tag{15}$$

The Jacobian matrix $\mathbf{J}(\mathbf{q})$ with size $3 \times 3n$ is presented

$$\mathbf{J}(\mathbf{q}) = \begin{bmatrix} J_{11} & J_{12} & J_{13} & J_{14} & .... & J_{1(3n)} \\ J_{21} & J_{22} & J_{23} & J_{24} & .... & J_{2(3n)} \\ J_{31} & J_{32} & J_{33} & J_{34} & .... & J_{3(3n)} \end{bmatrix} \tag{16}$$

The multi-section spatial continuum robot is the redundant system. The inverse kinematic problem for a redundant robot has multiple solutions in general. Due to the non-square Jacobian matrix for $3n$ DOFs robot, the basic inverse solution to (15) is obtained by using the pseudoinverse $\mathbf{J}^*$ of the matrix $\mathbf{J}$ and the inverse solution can then be written as [22]

$$\dot{\mathbf{q}} = \mathbf{J}^*(\mathbf{q})\dot{\mathbf{x}} \tag{17}$$

where, the pseudoinverse $\mathbf{J}^*$ can be computed as

$$\mathbf{J}^* = \mathbf{J}^T(\mathbf{J}\mathbf{J}^T)^{-1} \tag{18}$$

A common method of including the null space in a solution is the formulation in [22], [23] and the general inverse solution can be described as

$$\dot{\mathbf{q}} = \mathbf{J}^*(\mathbf{q})\dot{\mathbf{x}} + (\mathbf{I} - \mathbf{J}^*(\mathbf{q})\mathbf{J}(\mathbf{q}))\dot{\mathbf{q}}_0 \tag{19}$$

where, $\mathbf{I}$ is the unit matrix with size $3n \times 3n$ and $\mathbf{q}_0$ is the initial joint vector. Open-loop solutions of joint variables through numerical integration unavoidably lead to errors in workspace [22]. In order to overcome these drawbacks, the closed-loop algorithm is used based on the path error $\mathbf{e}$ in workspace between the desired and actual path. Consider the location error $\mathbf{e}$ and its derivative $\dot{\mathbf{e}}$ which can be given as

$$\mathbf{e} = \mathbf{x}_d - \mathbf{x}; \dot{\mathbf{e}} = \dot{\mathbf{x}}_d - \dot{\mathbf{x}} \tag{20}$$

The generalized closed-loop inverse kinematic algorithm can be expressed by [22], [23]

$$\dot{\mathbf{q}} = \mathbf{J}^*(\mathbf{q})(\dot{\mathbf{x}}_d + \mathbf{K}_p(\mathbf{x}_d - \mathbf{x})) \qquad (21)$$

Combining (15) and (21) together, there will be

$$\dot{\mathbf{e}} + \mathbf{K}_p\mathbf{e} = 0 \qquad (22)$$

where, $\mathbf{K}_p$ is a symmetric positive definite matrix.

Combining (19) and (22) together, the inverse kinematic solution of redundant robot based on closed-loop

algorithm is given as

$$\dot{\mathbf{q}} = \mathbf{J}^*(\mathbf{q})(\dot{\mathbf{x}}_d + \mathbf{K}_p(\mathbf{x}_d - \mathbf{x})) + (\mathbf{I} - \mathbf{J}^*(\mathbf{q})\mathbf{J}(\mathbf{q}))\dot{\mathbf{q}}_0 \qquad (23)$$

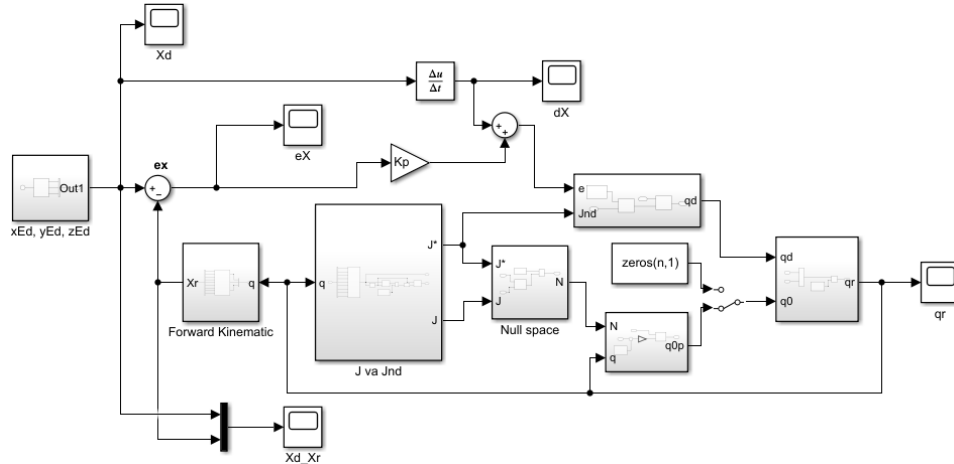Perform the algorithm in MATLAB/SIMULINK environment as Fig. 9.



Figure. 9. Inverse kinematic solution in MATLAB/SIMULINK

Apply the inverse kinematic algorithm for a spatial three-section continuum robot with the desired path as

$$\begin{cases} x_E = 0.6 + 0.2\sin(t) \quad (m) \\ y_E = 0.1 + 0.5\cos(t) \quad (m) \\ z_E = 0.4 - 0.1\cos(t) \quad (m) \end{cases} \qquad (24)$$

The desired position and velocity of end-effector are shown as Fig. 10 and Fig. 11. The simulation results are described from Fig. 12 to Fig. 15. Fig. 12 shows the curvatures of sections. The maximum curvature of sections sequence are $2.25(m^{-1})$, $2(m^{-1})$ and $1.5(m^{-1})$. The larges the curvature value, the smaller the radius of arc value. Fig. 13 describes the bending angle in the bending plane $OXZ$, respectively. The maximum bending angle of sections are $0.4(rad), 1.7(rad)$ and $0.25(rad)$. The orientation angles of sections are shown in Fig. 14. The location errors values of end-effector on axes $(OX)_0, (OY)_0$ and $(OZ)_0$ are presented in Fig. 15.
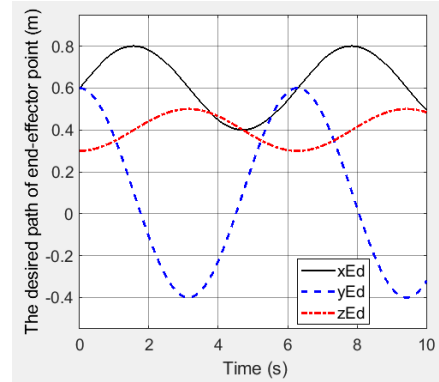


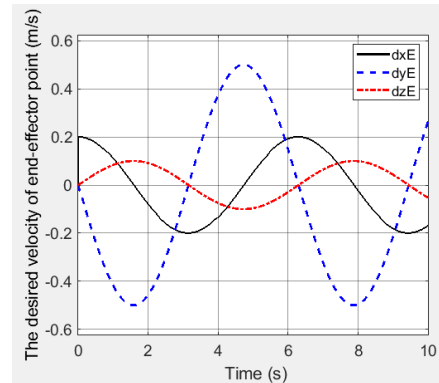Figure 10. The desired endpoint path in the workspace



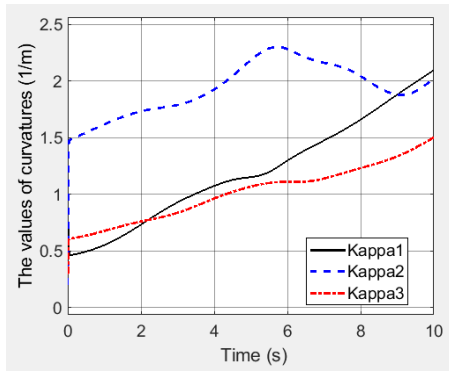Figure 11. The desired endpoint velocity in the workspace

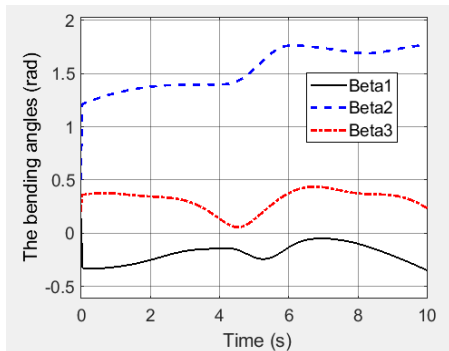Figure 12. The curvature values of three sections

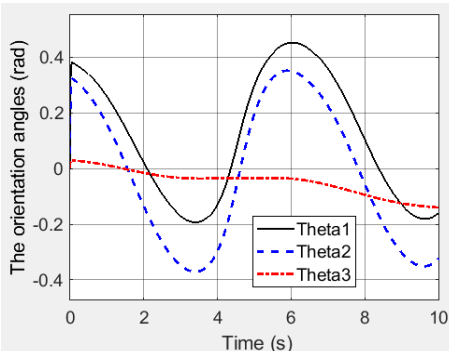

Figure 13. The bending angle values of three sections



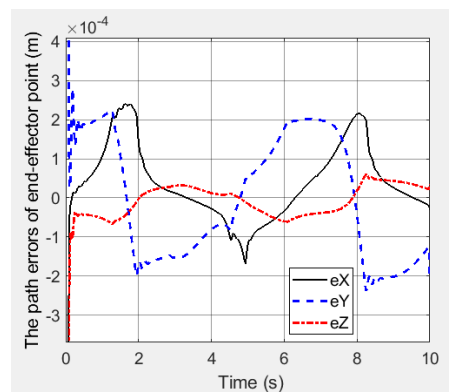Figure 14. The orientation angle values of three sections



Figure 15. The path error of endpoint in workspace

## 4. Conclusion

The motion of continuum robots is generated through the bending of the robot over a given section unlike traditional robots where the motion occurs in discrete location, i.e., joints. This paper considers analyzing kinematic modeling of the spatial multi-section continuum robots based on some specific assumptions. The forward and inverse kinematics problem of a spatial three-section continuum robot are solved as the illustrative example. The simulation results of inverse kinematic applying closed-loop algorithm for a three-section spatial continuum robot show high efficiency and small errors. The results of this research can be generalized for other continuum robot such as varied multi-section robot, more numbers of degree of freedom and build the dynamics equations and design the control system.

## 5. References

[1] B. K. Jessica, D. C. Rucker (2015) *Continuum Robots for Medical Applications: A Survey*. Transactions on robotics, DOI: 10.1109/TRO.2015.2489500

[2] M. B. Wooten, I. D. Walker (2018) *Vine-Inspired Continuum Tendril Robots and Circumnutations*. Robotics, vol. 7, no. 58, pp. 2-16.

[3] F. Renda, M Giorelli, M. Calisti, M Cianchetti, C. Laschi (2014) *Dynamic Model of a Multibending Soft Robot Arm Driven by Cables*. IEEE Trasactions on robotics, pp. 1-14.

[4] Y. Liu, J. Chen, J. Liu (2018) *Nonlinear mechanics of flexible cables in space robotic arms subject to complex physical environment*. Nonlinear dynamic.

[5] Y. Han, L. Zhou, W. Xu (2019) A comprehensive static model of cable-driven multi-section continuum robots considering friction effect. Mechanism and Machine Theory, vol. 135, pp. 130-149.

[6] Amouri, C. Mahfoudi, S. Djeffal (2019) *Kinematic a nd Dynamic Modeling and S imulation Analysis of a cable-driven continuum robot*. Computational Methods and Experimental Testing in Mechanical Engineering, pp. 27-37.

[7] D. C. Rucker, R. J. Webster (2011) *Statics and Dynamics of Continuum Robots with General Tendon Routing and External Loading*. Transactions on robotics, vol. 27, no. 6, pp. 1033-1044.

[8] S. R. William, P. B. Tzvi (2014) *Continuum Robot Dynamics Utilizing the Principle of Virtual Power*. Transactions on robotics, vol. 30, no. 1, pp. 275-287.

[9] L. Zheng, W. Liao, R. Hongliang, Y. Haoyong (2017) *Kinematic comparison of surgical tendon-driven*

manipulators and concentric tube manipulators. Mechanism and Machine Theory, vol. 107, pp. 148-165.

[10] Mukherjee, A. Senpupta, S. Bhaumik (2018) *Kinematics and Teleoperation of Tendon Driven Continuum Robot*. International Conference on Robotics and Smart Manufacturing (RoSMa2018), vol. 138, pp. 879-886.

[11] M. B. Wooten, I. D. Walker (2018) *Vine-Inspired Continuum Tendril Robots and Circumnutations*. Robotics, vol. 7, no. 58, pp. 2-16.

[12] G. Ian, D. R. Chris and I. D. Walker (2003) *Large Deflection Dynamics and Control for planar Continuum robot*. IEEE/ASME Transactions on mechatronics, vol. 8, no. 2, pp. 299-307.

[13] Kai Xu, S. Nabil (2010) Analytic Formulation for Kinematics, Statics, and Shape Restoration of Multi-backbone continuum Robots Via Elliptic Integrals. Journal of mechanism and robotics, vol. 2, pp. 1-13.

[14] T. John, D. C. Rucker (2016) *Elastic Stability of Cosserat Rods and Parallel Continuum Robots*. Transactions on robotics, DOI: 10.1109/TRO.2017.2664879.

[15] Ahmad, S. Khoo, M. Norton (2019) *Robust control of continuum robots using Cosserat rod theory*. Mechanism and Machine Theory, vol. 131, pp. 48-61.

[16] T. John, A. Vincent, C. Rucker (2019) *Real-Time Dynamics of Soft and Continuum Robots based on Cosserat-Rod Models*. The International Journal of Robotics Research, DOI: 10.1177/ToBeAssigned.

[17] S. M. H. Sadati, S. E. Naghibi, A. Shiva, I. D. Walker, K. Althofer, T. Nanayakkara (2017) *Mechanics of continuum Manipulators, A Comparative Study of Five Methods with Experiments*. Conference Paper *in* Lecture Notes in Computer Science. DOI: 10.1007/978-3-319-64107-2_56.

[18] B. A. Jones, I. D. Walker (2006) *Kinematics for Multi-section Continuum Robots*. IEEE/ASME Transactions on mechatronics, vol. 22, no. 1, pp. 43-55.

[19] L. Othman, A. Melingui, A. Chibani, C. Escande, R. Merzouki (2014) *Inverse Kinematic Modeling of a class of Continuum Bionic Handling Arm*. Proceedings of the International conference on advanced intelligent mechatronics, France.

[20] S. Inderjeet, L. Othman, A. Yacine, C. incent, P. M. Pushparaj, M. Rochdi (2017) *Performances Evaluation of Inverse Kinematic Models of a Compact Bionic Handling Assistant*. Proceedings of the 2017 IEEE International Conference on robotics and biomimetics, Macau, China.

[21] W. Zhang, Z. Yang, T. Dong, Kai Xu (2018) *FABRIKc: An Efficient Iterative Inverse Kinematics Solver for Continuum Robots*. Proceedings of the 2018 IEEE/ASME International Conference on Advanced Intelligent Mechatronics (AIM), Auckland, New Zealand.

[22] F. Fahimi (2009) Autonomous Robots – Modeling, path planning and control. Hardcover, Springer.

[23] R. J. Webster and B. A. John (2010) *Design and Kinematic Modeling of Constant Curvature Continuum Robots: A Review*. The International Journal of Robotics Research, pp. 1-22, DOI: 10.1177/0278364910368147.